ChemComm
RSC Publishing

COMMUNICATION
View Article Online
View Journal

Cite this: DOI: 10.1039/c3cc42121j

Received 24th March 2013,
Accepted 7th May 2013

DOI: 10.1039/c3cc42121j

www.rsc.org/chemcomm

New triphenylamine organic dyes containing dithieno[3,2-*b*:2′,3′-*d*]pyrrole (DTP) units for iodine-free dye-sensitized solar cells†

Zhihui Wang,[a] Mao Liang,*[b] Lina Wang,[b] Yujie Hao,[b] Chunbo Wang,[b] Zhe Sun[b] and Song Xue*[b]

Three dithieno[3,2-*b*:2′,3′-*d*]pyrrole (DTP) units with different hexyloxyphenyl (HOP) substituents have been developed for triphenylamine organic dyes (XS54–XS56). The introduction of the 4-HOP-DTP unit has resulted in a stronger light harvesting capacity, accounting for the observed photocurrent enhancement in the case of XS54, while the 2-HOP-DTP/2,4-HOP-DTP units induce a strikingly large photovoltage improvement in the cases of XS55 and XS56 due to their higher steric hindrance.

During the past two decades, numerous research attempts have been made to explore new photosensitizers (*e.g.* Ru-based complexes,[1] zinc porphyrin complexes[2] and organic sensitizers[1–3]) and iodine-free redox couples[4] as well as to understand in-depth essential interface processes[5] in the development of dye-sensitized solar cells (DSCs). Amongst the various classes of emerging photosensitizers, organic sensitizers with robust availability, ease of structural tuning and generally high molar extinction coefficients have recently received great attention.

Studies have shown that development of new fused-ring building blocks as spacers is an effective strategy for obtaining highly efficient organic sensitizers.[1] Representative fused-ring thiophenes reported in the literature include benzodithiophenes (benzo[1,2-*b*:4,5-*b*′]-dithiophene, BDT1;[6] benzo[2,1-*b*:3,4-*b*′] dithiophene, BDT2[6]) and β,β′-bridged bithiophenes (dithieno[3,2-*b*:2′,3′-*d*]silole, DTS;[7] cyclopentadithiophene, **CPDT**;[8] dithieno[3,2-*b*:2′,3′-*d*]pyrrole, **DTP**[9]). It is valuable to note that organic dyes featuring the alkyl-functionalized **CPDT** bridge hold the record for validated efficiency of over 10%.[8] If a new fused-ring thiophene with a superior performance relative to **CPDT** is explored, new breakthroughs in the development of organic dyes would be expected. However, to the best of our knowledge, there are few reports on this issue.[10]

In this work, we report three triphenylamine dyes (**XS54–XS56**, Fig. 1) containing new **DTP** units, *i.e.* 4-hexyloxyphenyl-substituted **DTP** (4-HOP-DTP), 2-hexyloxyphenyl-substituted **DTP** (2-HOP-DTP) and 2,4-bis(hexyloxy)phenyl-substituted **DTP** (2,4-HOP-DTP). **XS57** featuring the dihexylcyclopentadithiophene (DH-CPDT) bridge was prepared as a reference. Device performance characteristics demonstrate the superiority of employing 4-HOP-DTP relative to DH-CPDT as the conjugated spacer in this type of organic dyes.

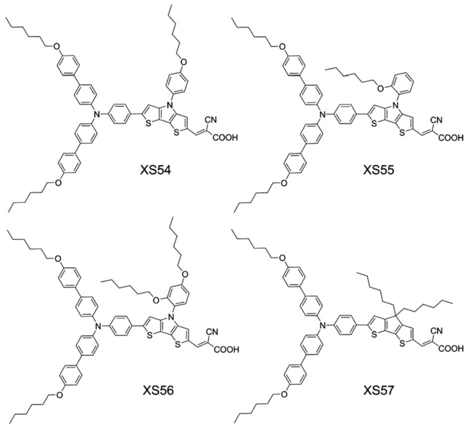

Fig. 1 Chemical structures of **XS54–57**.

The UV-vis absorption spectra of the dyes in CH_2Cl_2 solutions are depicted in Fig. 2a. The optical and electrochemical properties of the dyes are summarized in Table 1. The dye alteration from

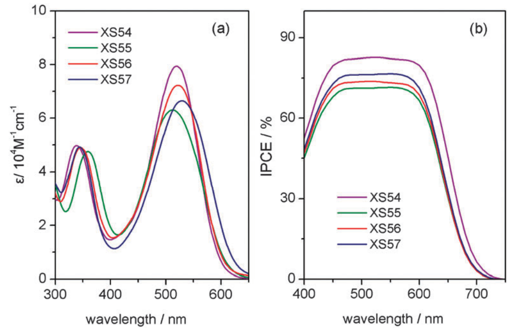

Fig. 2 (a) Absorption spectra of dyes in DCM; (b) IPCEs action spectra for DSCs employing the cobalt electrolyte.

---

[a] *Department of Chemistry, Tianjin University, Tianjin, 300072, P.R. China*
[b] *Department of Applied Chemistry, Tianjin University of Technology, Tianjin, 300384, P.R.China. E-mail: liangmao717@126.com, xuesong@ustc.edu.cn; Fax: +86 22 60214252; Tel: +86 22 60214250*

† Electronic supplementary information (ESI) available: Experimental details, Fig. S1–S6 and Tables S1–S3. See DOI: 10.1039/c3cc42121j

Table 1 Optical and electrochemical properties of the dyes

Dye	λ_{max}/nm (ε/10^3 M^{-1} cm^{-1})	E_{0-0} [a]/eV	$E_{D/D+}$ [b]	$E_{D*/D+}$ [c]
XS54	338 (53), 520 (79.9)	2.17	0.97	−1.20
XS55	359 (47), 510 (63.4)	2.19	1.00	−1.19
XS56	346 (45), 522 (72.5)	2.17	1.01	−1.16
XS57	344 (43), 529 (66.8)	2.12	0.99	−1.13

[a] E_{0-0} values were estimated from the intersections of normalized absorption and emission spectra (Fig. S1, ESI). [b] First oxidation potentials (*vs.* NHE) of dye-loaded films internally calibrated with ferrocene (0.63 V *vs.* NHE). [c] $E_{D*/D+}$ were calculated from $E_{D*/D+} = E_{D/D+} - E_{0-0}$.

Table 2 Photovoltaic performance of DSCs employing the cobalt electrolyte under AM 1.5 irradiation[a]

Dyes	J_{SC}/mA cm^{-2}	V_{OC}/mV	FF	PCE%	Γ/10^{-7}mol cm^{-2}
XS54	13.5	850	0.71	8.14	0.76
XS55	11.2	950	0.70	7.45	0.36
XS56	11.6	935	0.69	7.48	0.97
XS57	12.1	907	0.70	7.68	0.46

[a] Thin film (5 μm) was used to fabricate the devices with an active surface area of 0.156 cm^2.

XS55 (510 nm) to **XS54** (520 nm) has caused a λ_{max} red-shift of 10 nm along with enhanced maximum molar absorption coefficients (ε), indicating that the electron density of 4-HOP-DTP is higher than that of 2-HOP-DTP. This observation can be understood from molecular modeling studies of **XS54** and **XS55** (Fig. S2, ESI†). Theoretical computation shows that the ground state structure of **XS54** possesses a 49° twist between the 4-HOP and the **DTP** skeleton, while the corresponding dihedral angle in **XS55** is larger, with the value being 62°. Therefore, the red shift of the absorption band of **XS54** is predominantly caused by a more planar conjugating system. Although **XS54** displays a slight blue shift of λ_{max} as compared to **XS57**, a higher maximum molar absorption coefficient is observed for the former, which is desirable for thin-layer DSCs.

Cyclic voltammetry (CV) was carried out in a typical three-electrode electrochemical cell with TiO$_2$ film stained with sensitizers as the working electrode (Fig. S3, ESI†). **XS54** exhibits the lowest HOMO level of 0.97 V *vs.* NHE among the three dyes, which is even lower than that of **XS57** (0.99 V *vs.* NHE), indicating the stronger electron-donating capability of the 4-HOP-DTP unit. The driving forces for dye regeneration of **XS54–XS56** are around 0.37 eV, which is close to that of **XS57**. On the other hand, the driving forces for electron injection of **XS54–XS56** (0.66–0.7 eV) are larger than that of **XS57** (0.63 eV).

As shown in Fig. 3, we recorded the photocurrent density–voltage (*J–V*) curves of the devices employing a tris(1,10-phenanthroline)cobalt(II/III) redox shuttle under AM 1.5 irradiation (100 mW cm^{-2}), and the detailed parameters are collected in Table 2. The cobalt electrolyte is composed of 0.25 M [Co(II)(phen)$_3$](PF$_6$)$_2$, 0.05 M [Co(III)(phen)$_3$](PF$_6$)$_3$, 0.5 M 4-tert-pyridine (TBP) and 0.1 M lithium bis-(trifluoromethanesulfonyl)-imide (LiTFSI) in acetonitrile.[11] A typical cell based on **XS54** has a short-circuit photocurrent density (J_{SC}) of 13.5 mA cm^{-2}, an open-circuit photovoltage (V_{OC}) of 850 mV and a fill factor (FF) of 0.71, affording a PCE of 8.14%. There is 17.8% enhancement in J_{SC} of **XS54** in comparison with **XS55** (11.2 mA cm^{-2}) in the cobalt cells. Moreover, it is also valuable to note that **XS54** possesses noticeably enhanced J_{SC} relative to that of its **CPDT** congener (**XS57**, 12.1 mA cm^{-2}), suggesting that the pursuit of fused-ring thiophene with high electron-donating ability is a rational strategy for J_{SC} optimization. The J_{SC} enhancement of **XS54**, mainly benefiting from its broad and high IPCE action area (Fig. 2b), can be attributed to its stronger molar absorption coefficients (Table 1) and higher amounts of the dyes adsorbed (Table 2). Evidently, the remarkably improved J_{SC} of **XS54** significantly contributes to its PCE values. As a result, **XS54** sensitized DSCs employing the cobalt electrolyte yield the highest efficiency amongst these four dyes. Note that there is no scattering layer used in the fabrication of DSCs, which is one of the main reasons that the performance of DSCs shown in this work is not higher than that reported in the literature. However, in view of the same conditions of the test, our approach is reliable for fair evaluation of the photovoltaic performance of the four dyes discussed in this work. Three batches of cells were fabricated and these results confirm that for the [Co(II/III)(phen)$_3$](PF$_6$)$_{2/3}$ redox shuttle, **XS54** featuring the 4-HOP-DTP spacer outperforms the DH-CPDT counterpart, **XS57**.

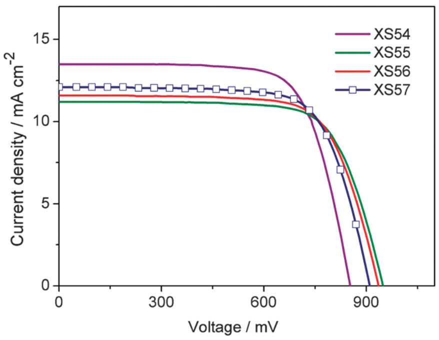

Fig. 3 *J–V* characteristics of DSCs employing the cobalt electrolyte.

Apart from the photocurrent, the position of hexyloxyl also has a distinct impact on the photovoltage of the devices. Surprisingly, the superior performance of 2-HOP-DTP as a π-linker relative to 4-HOP-DTP in terms of the V_{OC} is particularly noteworthy. Compared with **XS54**, the introduction of the 2-HOP group into the **DTP** unit in **XS55** successfully realizes a significant increase in V_{OC} by 100 mV. The positive impact of 2-HOP-DTP on the V_{OC} of devices can also be found in the case of **XS56**, which exhibits a high V_{OC} of 935 mV. The photovoltaic characteristics of **XS56** show a slightly decreased J_{SC} value as for **XS57**, while the V_{OC} is 28 mV higher, resulting in a comparable PCE value of 7.48%.

To clarify the origin of the observed V_{OC} improvement upon the employment of the photosensitizers featuring a 2-HOP-DTP/2,4-HOP-DTP, we focus on the dyes with the most contrasting photovoltages, *i.e.* **XS54** and **XS55**. As commonly understood, V_{OC} is intimately correlated to the conduction band (CB) position and the charge recombination rate.[12,13] Fig. 4a shows the relationship between V_{OC} and extracted charge density (Q) at open circuit potential. At a fixed Q, the higher V_{OC} value of **XS54** relative to **XS55** indicates a negative shift of the CB.[14]

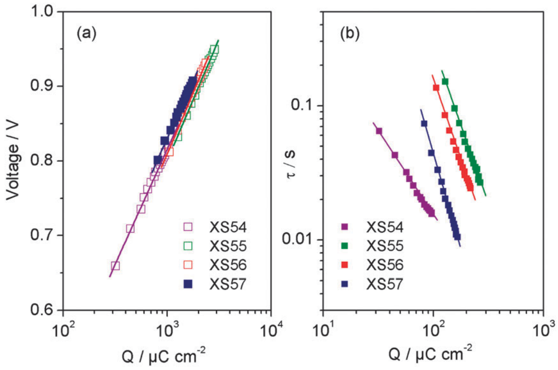

Fig. 4 Charge density at open circuit potential (a) and electron lifetime (b) as a function of voltage for DSCs.

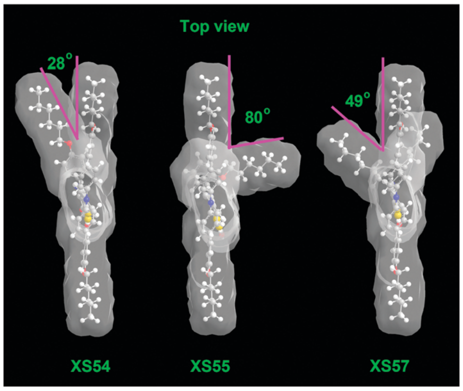

Fig. 5 Optimized geometries of **XS54**, **XS55** and **XS57**.

Compared to **XS54**, **XS55** showed a downward CB shift by 14 mV. That is to say, the positive shift of the CB of **XS55** should cause a V_{OC} attenuation of 14 mV, in sharp contrast to a 100 mV enhancement as demonstrated by photovoltaic characteristics. Therefore, we can arrive at a conclusion that the observed higher V_{OC} for **XS55** should be attributed to the retarded charge recombination, which benefits the cell photovoltage more than 100 mV. Fig. 4b shows the electron lifetime against charge density for DSCs based on **XS54** and **XS55**. At matched electron density, the electron lifetime of the **XS55** sensitized DSC is much longer than that of **XS54**. This indicates that charge recombination between electrons in TiO_2 film and electron acceptors in the electrolyte is significantly retarded by the 2-HOP-DTP unit as compared to the 4-HOP-DTP unit.

Interestingly, based on the data of Fig. 4, the voltage advantage of **XS55** over **XS57** can also be ascribed to the retarded charge recombination rather than the shift of the CB. The ability to retard charge recombination is therefore suggested to be determined by the direction of alkyl chains rather than the number of the alkyl chains. As presented in Fig. 5, the angles between the alkyl chain and the molecular skeleton from the top view of **XS54**, **XS55** and **XS57** were estimated to be 28°, 80° and 49°, respectively. A larger angle indicates the increasing steric hindrance, which blocks the approach of the Co(III) ions to TiO_2 film. Obviously, the 3D structure of **XS55** is favorable for retarding charge recombination.

In summary, three **DTP** based triphenylamine sensitizers have been designed and synthesized. Despite the slight blue shift of absorption, **XS54** has a relatively high IPCE mainly due to stronger molar absorption coefficients and higher amounts of the dyes adsorbed on TiO_2. In conjunction with the cobalt electrolyte, **XS54** featuring the 4-HOP-DTP spacer yields a PCE of 8.14%, outperforming the analogous device constructed using **XS57**. Furthermore, electron lifetime studies show that charge recombination rates are suggested to be determined by the direction of alkyl chains rather than the number of the alkyl chains. These findings will considerably encourage further molecular engineering of low-cost organic dyes for DSCs.

The authors acknowledge financial support from the National Natural Science Foundation of China (21003096, 21072152, 21103123).

Notes and references

1 (*a*) A. Hagfeldt, G. Boschloo, L. Sun, L. Kloo and H. Pettersson, *Chem. Rev.*, 2010, **110**, 6595–6663; (*b*) Y.-S. Yen, H.-H. Chou, Y.-C. Chen, C.-Y. Hsu and J. T. Lin, *J. Mater. Chem.*, 2012, **22**, 8734–8747.

2 (*a*) L.-L. Li and E. W.-G. Diau, *Chem. Soc. Rev.*, 2013, **42**, 291–304; (*b*) M. J. Griffith, K. Sunahara, P. Wagner, K. Wagner, G. G. Wallace, D. L. Officer, A. Furube, R. Katoh, S. Mori and A. J. Mozer, *Chem. Commun.*, 2012, **48**, 4145–4162; (*c*) Y. Liu, H. Lin, J. T. Dy, K. Tamaki, J. Nakazaki, D. Nakayama, S. Uchida, T. Kubo and H. Segawa, *Chem. Commun.*, 2011, **47**, 4010–4012.

3 (*a*) M. Velusamy, K. R. J. Thomas, J. T. Lin, Y. C. Hsu and K. C. Ho, *Org. Lett.*, 2005, **7**, 1899–1902; (*b*) Y. Oyama, S. Inoue, T. Nagano, K. Kushimoto, J. Ohshita, I. Imae, K. Komaguchi and Y. Harima, *Angew. Chem., Int. Ed.*, 2011, **50**, 7429–7433.

4 (*a*) M. K. Kashif, J. C. Axelson, N. W. Duffy, C. M. Forsyth, C. J. Chang, J. R. Long, L. Spiccia and U. Bach, *J. Am. Chem. Soc.*, 2012, **134**, 16646–16653; (*b*) Y. Xie and T. W. Hamann, *J. Phys. Chem. Lett.*, 2013, **4**, 328–332; (*c*) S. Ahmad, T. Bessho, F. Kessler, E. Baranoff, J. Frey, C. Yi, M. Grätzel and M. K. Nazeeruddin, *Phys. Chem. Chem. Phys.*, 2012, **14**, 10631–10639.

5 E. Mosconi, J.-H. Yum, F. Kessler, C. J. G. García, C. Zuccaccia, A. Cinti, M. K. Nazeeruddin, M. Grätzel and F. D. Angelis, *J. Am. Chem. Soc.*, 2012, **134**, 19438–19453.

6 (*a*) X. Hao, M. Liang, X. Cheng, X. Pian, Z. Sun and S. Xue, *Org. Lett.*, 2011, **13**, 5424–5427; (*b*) P. Gao, H. N. Tsao, M. Grätzel and M. K. Nazeeruddin, *Org. Lett.*, 2012, **14**, 4330–4333; (*c*) E. Longhi, A. Bossi, G. Di Carlo, S. Maiorana, F. De Angelis, P. Salvatori, A. Petrozza, M. Binda, V. Roiati, P. R. Mussini, C. Baldoli and E. Licandro, *Eur. J. Org. Chem.*, 2013, 84–94.

7 W. Zeng, Y. Cao, Y. Bai, Y. Wang, Y. Shi, M. Zhang, F. Wang, C. Pan and P. Wang, *Chem. Mater.*, 2010, **22**, 1915–1925.

8 (*a*) H. N. Tsao, J. Burschka, C. Yi, F. Kessler, M. K. Nazeeruddin and M. Grätzel, *Energy Environ. Sci.*, 2011, **4**, 4921–4924; (*b*) H. N. Tsao, C. Y. Yi, T. Moehl, J. H. Yum, S. M. Zakeeruddin, M. K. Nazeeruddin and M. Grätzel, *ChemSusChem*, 2011, **4**, 591–594; (*c*) Y. M. Cao, N. Cai, Y. L. Wang, R. Z. Li, Y. Yuan and P. Wang, *Phys. Chem. Chem. Phys.*, 2012, **14**, 8282–8286.

9 (*a*) M. F. Xu, M. Zhang, M. Pastore, R. Z. Li, F. D. Angelis and P. Wang, *Chem. Sci.*, 2012, **3**, 976–983; (*b*) N. Cai, J. Zhang, M. Xu, M. Zhang and P. Wang, *Adv. Funct. Mater.*, 2013, DOI: 10.1002/adfm.201203348; (*c*) J. Zhang, Z. Yao, Y. Cai, L. Yang, M. Xu, R. Li, M. Zhang, X. Dong and P. Wang, *Energy Environ. Sci.*, 2013, **6**, 1604–1614.

10 M. Liang and J. Chen, *Chem. Soc. Rev.*, 2013, **42**, 3453–3488.

11 X. P. Zong, M. Liang, T. Chen, J. N. Jia, L. N. Wang, Z. Sun and S. Xue, *Chem. Commun.*, 2012, **48**, 6645–6647.

12 T. Marinado, K. Nonomura, J. Nissfolk, M. K. Karlsson, D. P. Hagberg, L. Sun, S. Mori and A. Hagfeldt, *Langmuir*, 2010, **26**, 2592–2598.

13 E. Ronca, M. Pastore, L. Belpassi, F. Tarantelli and F. De Angelis, *Energy Environ. Sci.*, 2013, **6**, 183–193.

14 N. Kopidakis, N. R. Neale and A. J. Frank, *J. Phys. Chem. B*, 2006, **110**, 12485–12489.